

## TWO-PHOTON ANNIHILATION OF THERMAL PAIRS IN STRONG MAGNETIC FIELDS

MATTHEW G. BARING  
Department of Physics  
North Carolina State University  
and

ALICE K. HARDING  
Laboratory for High Energy Astrophysics  
NASA/Goddard Space Flight Center

### ABSTRACT

The annihilation spectrum of pairs with one-dimensional thermal distributions in the presence of a strong magnetic field is calculated. Numerical computations of the spectrum are performed for mildly relativistic temperatures and for different angles of emission with respect to field lines. Teragauss magnetic fields are assumed so that conditions are typical of gamma-ray burst and pulsar environments. The spectra at each viewing angle reveal asymmetric line profiles that are signatures of the magnetic broadening and redshifting of the line: these asymmetries are more prominent for small viewing angles. Thermal Doppler broadening tends to dominate in the right wing of the line and obscures the magnetic broadening more at high temperatures and smaller viewing angles. This angular dependence of the line asymmetry may prove a valuable observational diagnostic tool. For low temperatures and magnetic field strengths useful analytic expressions are presented for the line width, and also for the annihilation spectrum at zero viewing angle. The results presented find application in gamma-ray burst and pulsar models, and may prove very helpful in deducing field strengths and temperatures of the emission regions of these objects from line observations made by Compton/GRO and future missions.

### INTRODUCTION

There is substantial observational motivation for detailed calculations of the annihilation spectrum of thermal pairs in the presence of a strong magnetic field. If the features observed around 400 keV in gamma-ray burst (GRB) spectra (see Mazets *et al.*, 1981) are interpreted as red-shifted 511 keV lines (for an extensive list of observations see Liang, 1986), then pair annihilation is taking place near a neutron star surface and will thus be influenced by a strong magnetic field. Further, recent observations (see Agrinier *et al.*, 1990) by the FIGARO II experiment of an emission feature at about 400 keV in the spectrum of the Crab pulsar are suggestive of a red-shifted annihilation line in this neutron star source. A study of the influence that a strong magnetic field has on the annihilation spectrum is therefore of significant interest to astrophysicists.

There are two important effects of the magnetic field on two-photon pair annihilation: (i) because of the very high cyclotron emission rates, the vast majority of pairs will annihilation

late from the ground Landau state with a one-dimensional (1D) momentum distribution, and (ii) since transverse momentum is not conserved in a strong magnetic field, there is an intrinsic broadening of the two-photon annihilation line due to an increased availability of phase space for this interaction. These effects become significant when the magnetic field exceeds about a few percent of the quantum critical field  $B_c = m_e^2 c^3 / (e \hbar) = 4.413 \times 10^{13}$  Gauss, which corresponds to conditions in neutron star environments. To a first approximation, it is reasonable to assume that the annihilating pairs have a 1D thermal distribution. The effects of the field on the shape of the thermal annihilation spectrum are potentially the most useful observational diagnostic tool: the total rate of annihilation is not altered much by the presence of the field when  $B \lesssim 4 \times 10^{12}$  Gauss (Wunner, 1979).

Due to the intrinsic geometrical asymmetry imposed by the field, both the thermal and magnetic contributions to the width of the annihilation line will be very angle dependent. Intuitively, at viewing angles  $\theta_1 \sim 0^\circ$  to the field, thermal Doppler broadening is expected to be a maximum while magnetic broadening is a minimum. For viewing angles  $\theta_1 \sim 90^\circ$  to the field this situation is reversed so that the magnetic broadening should be more significant in comparison with the Doppler broadening. These expectations are borne out by the computational results that are presented here. The prediction that the width of observed lines at some angles could be due primarily to the magnetic field is observationally significant. Annihilation spectra produced by pairs with a 1D thermal distribution have been calculated by Kaminker *et al.* (1990), revealing significantly reduced Doppler broadening at  $\theta_1 \sim 90^\circ$ . However, they did not include the effects of magnetic broadening. In an earlier paper, Kaminker *et al.* (1987) presented spectra for the annihilation of pairs *at rest* in the presence of a field. Here we present the first calculation of two-photon annihilation spectra from a 1D thermal pair distribution, including full magnetic broadening effects using the QED second-order annihilation cross section of Daugherty and Bussard (1980, hereafter DB80). Of particular interest are the angle-dependent asymmetries of the line profiles introduced by field broadening, signatures that may be detectable by the *BATSE* instrument aboard the GRO mission and future high-resolution detectors (e.g. *TGRS* and *NAE*).

## MAGNETIC TWO-PHOTON ANNIHILATION

It is convenient to use a simple dimensionless notation for various quantities in relativistic magnetized environments, in order to express analytic results more compactly. Hereafter, all magnetic fields will be expressed in units of the critical field  $B_c$ , and the parallel pair temperature parameter  $T$  will represent the quantity  $k_B T_e / (m_e c^2)$ , where  $k_B$  is Boltzmann's constant. All photon and particle energies and momenta will be scaled by  $m_e c^2$  and  $m_e c$ , respectively.

The conservation relations for energy and also for momentum parallel to the magnetic field during pair annihilation can be simply written down. Let  $p_- m_e c$  and  $p_+ m_e c$  be the momenta of the annihilating electron and positron, oppositely directed along the field, and  $\epsilon_- m_e c^2$  and  $\epsilon_+ m_e c^2$  be their energies. The produced photons have energies  $\omega_1 m_e c^2$  and  $\omega_2 m_e c^2$ , and propagate at angles  $\theta_1$  and  $\theta_2$  to the field. Using the abbreviated notation

$c_i = \cos \theta_i$ ,  $s_i = \sin \theta_i$ ,  $i = 1, 2$ , the conservation relations are

$$\begin{aligned}\varepsilon_- + \varepsilon_+ &= \omega_1 + \omega_2 \\ p_- - p_+ &= \omega_1 c_1 + \omega_2 c_2\end{aligned}\quad (1)$$

Alternatively these relations can be expressed in terms of the solutions for the pair momenta  $p_{\pm}$  (see DB80). The kinematical requirement that these momenta be real gives a restriction on the energy-angle phase space of the emitted photons:

$$\left| \omega_1 c_1 + \omega_2 c_2 \right| \leq \sqrt{(\omega_1 + \omega_2)^2 - 4} \quad (2)$$

For the annihilation of pairs with momenta  $p_{\pm} m_e c$  along the field, the distribution function for the pairs that is needed for the computation of thermal annihilation spectra can be obtained from equation (23) of Harding (1986):

$$\eta_{\pm}(p_{\pm}) = \frac{1}{2K_1(1/T)} \exp\left\{-\frac{\varepsilon_{\pm}}{T}\right\} \quad (3)$$

where  $T$  is the dimensionless temperature of the pairs and  $K_1$  is a modified Bessel function. The thermal annihilation spectrum can then be calculated by inserting this into the expression in eq. (24) of DB80, who performed the QED calculation for the annihilation cross-section from first principles. Their result is too small by a factor of two (c.f. Wunner, 1979), and also contains some minor typographical errors. The corrected annihilation spectrum taken from DB80 is then

$$R_{2\gamma}(\omega_1) = \int_{-\infty}^{\infty} \frac{dp_-}{\varepsilon_-} \int_{-\infty}^{\infty} \frac{dp_+}{\varepsilon_+} \int_0^{2\pi} d\phi_2 Q_{2\gamma} \quad (4a)$$

where

$$Q_{2\gamma} = \frac{n_+ n_-}{4K_1^2(1/T)} \frac{\alpha_f^2 \lambda_c^2}{32\pi} \frac{\omega_1}{B} \exp\left\{-\frac{\omega_1^2 s_1^2 + \omega_2^2 s_2^2}{2B} - \frac{\varepsilon_- + \varepsilon_+}{T}\right\} \sum_{\text{pol}} |\mathcal{M}|^2 \quad (4b)$$

Here  $\alpha_f \approx 1/137$  is the fine structure constant,  $\lambda_c = \hbar/(m_e c)$  and  $n_{\pm}$  are the particle number densities. The matrix element  $\mathcal{M}$  can be obtained from the results of DB80. The sum is over the polarization states of the photons.

In obtaining eq. (4) a change of variables was performed: the energy  $\omega_2$  and angle  $\theta_2$  of the unobserved photon were expressed in terms of the momenta  $p_{\pm}$  of the pairs via eq. (1). This transformation is convenient for both numerical and analytic computations, yielding simple integration limits: with it is associated a Jacobian given by  $\omega_2 d\omega_2 dc_2 = |p_- \varepsilon_+ + p_+ \varepsilon_-|/(\varepsilon_- \varepsilon_+) dp_- dp_+$ . The azimuthal angle  $\phi_2$  of the second photon is the third integration variable. In the limit of small  $\theta_1$ , the dominant contribution to the annihilation spectrum occurs when the exponential factor in eq. (4b) is maximized.

## NUMERICAL RESULTS

The results of numerical computations of the spectrum in eq. (4) are displayed in Figures 1–3. The principle magnetic effects are demonstrated in Fig. 1, where the pairs are assumed to be at rest, i.e. zero temperature. This corresponds to the case studied numerically by DB80 and Kaminker *et al.* (1987), and indeed the results presented in Fig. 1 are in close agreement with these earlier studies. With thermal broadening absent, Fig. 1 clearly illustrates the magnetic broadening effect in the left wing of the two-photon annihilation line. There are two prominent features to notice. First, the widths of the annihilation lines are dependent on the strength of the field and the angle of emission relative to field. These magnetic widths can be expressed approximately (for  $B \ll 1$ ) as

$$(\Delta\omega_1)^B \sim \begin{cases} B/2, & s_1 < \sqrt{2B}, \\ s_1\sqrt{B/2}, & s_1 > \sqrt{2B}, \end{cases} \quad (5)$$

remembering that  $s_1 = \sin\theta_1$ . These estimates can be obtained from eq. (4) or from the results of Kaminker *et al.* (1987). Second, observe the appearance of angular-dependent kinematic cutoffs, eliminating the right (blue) wing of the line. These occur at

$$\omega_1 = \frac{2}{1 + |c_1|}, \quad (6)$$

as can be determined from eq. (2). Due to the presence of this kinematic cutoff at  $\omega_1 > 1$ , most of the broadening occurs on the left (red) side of the line at angles other than  $90^\circ$ . Note that a summation of the spectra over emission angles removes the evidence of the line asymmetry and the kinematic cutoffs, producing a symmetric line profile.

The inclusion of thermal broadening for the case of finite  $T$  is illustrated in Figs. 2–3. The basic nature of Doppler broadening is similar to the 1D field-free case (Kaminker *et al.*, 1990), and the results show that the thermal contribution to the line broadening is greatest for small viewing angles. The first order contribution to the Doppler width is

$$(\Delta\omega_1)^D = c_1\sqrt{2T}, \quad (7)$$

when  $T \ll 1$ . The thermal broadening smooths out the line profile, and dominates the blue wing of the line, but evidence of the magnetically-broadened left wing remains for larger viewing angles. A comparison of eqs. (5) and (7) reveals that magnetic broadening will dominate over first-order Doppler broadening when

$$T \lesssim \begin{cases} 0.25 B s_1^2/c_1^2, & s_1 > \sqrt{2B}, \\ 0.125 B^2/c_1^2, & s_1 < \sqrt{2B}, \end{cases} \quad (8)$$

confirming the numerical spectral results that the Doppler mechanism is more effective at broadening the line for small viewing angles.

The calculations performed here are for conditions expected to be typical of gamma-ray burst or pulsar environments. It is anticipated that pairs in the ground state are likely to be in relatively cool quasi-thermal distributions. Cyclotron resonant scattering can

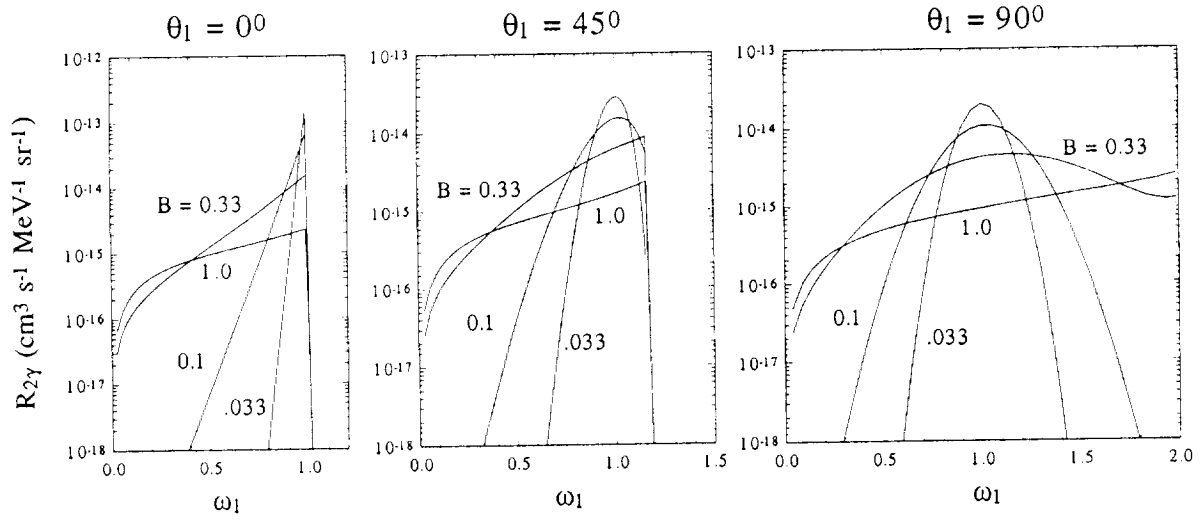


FIGURE 1 - Two-photon annihilation spectra for pairs at rest in the ground state, for different magnetic fields  $B$  and viewing angles  $\theta_1$  from numerical integration of the cross section over the energy  $\omega_2$  and angle  $\theta_2$  of the unobserved photon. The kinematic cutoffs occur when  $|\cos \theta_2| = 1$  (cf. Eq. 6).

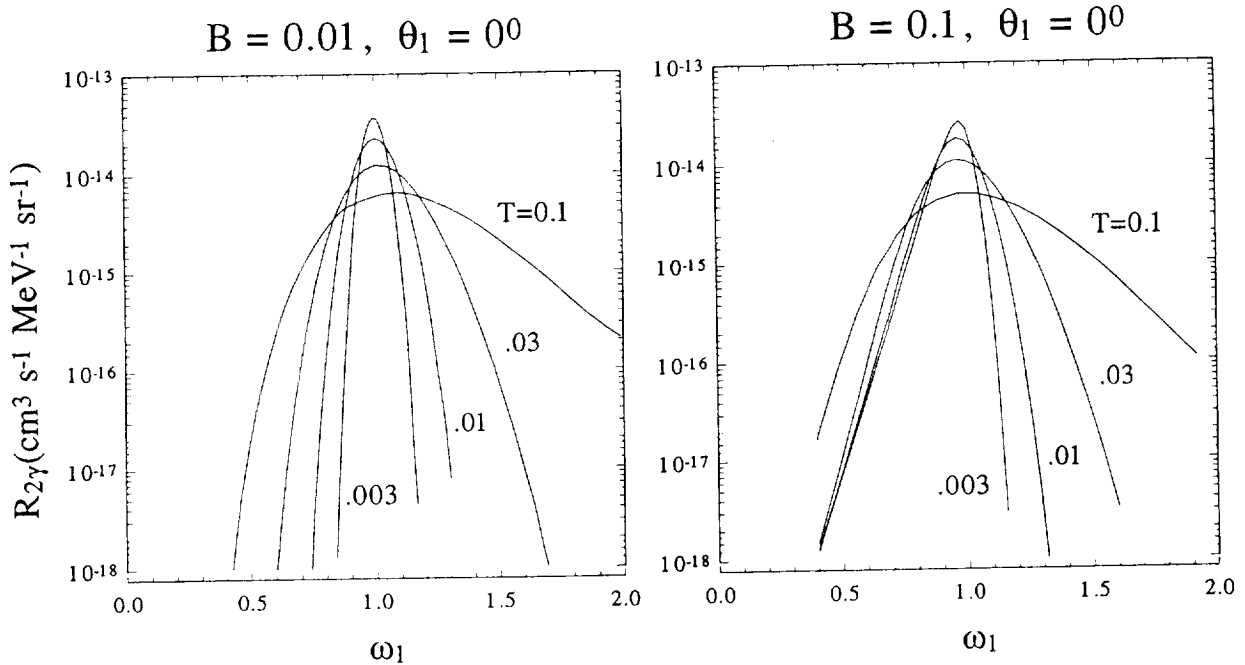


FIGURE 2 - Numerical annihilation spectra at an angle of  $0^\circ$  to the field direction for pairs in a 1D thermal distribution with parallel temperature  $T$  (in units of  $m_e c^2$ ) at two different field strengths.

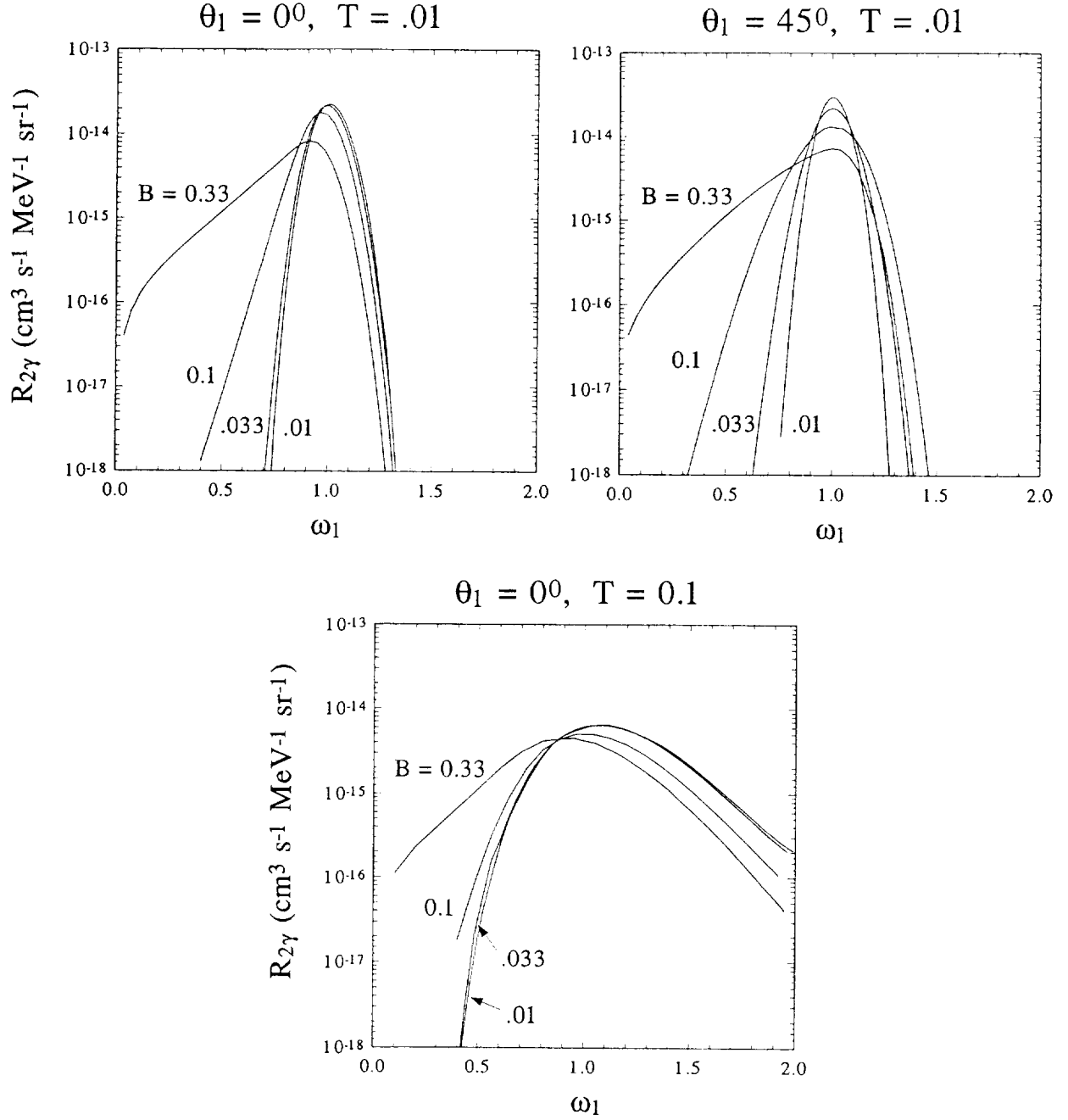


FIGURE 3 - Numerical annihilation spectra at different viewing angles  $\theta_1$  and parallel pair temperatures  $T$ , showing the effect of combined magnetic and thermal broadening.

cool pairs in the ground state before they annihilate (Preece and Harding, 1991) to temperatures  $T \sim B/4$  (Lamb *et al.*, 1990). In this case magnetic broadening is dominant for  $\tan^2 \theta_1 > 1$  or at viewing angles  $\theta_1 > 45^\circ$ . This angular effect shows significant potential as a spectral diagnostic for line observations in astrophysical sources.

## ANALYTIC SPECTRAL FORMS

It is useful to develop analytic approximations to the annihilation spectrum. These can be simply obtained in the low  $T$ , low  $B$  limit, and when the viewing angle is small:  $\theta_1 \approx 0^\circ$ . The integrations in eq. (4) are then analytically tractable because of the effective restriction to the  $\omega_2 - \cos \theta_2$  (or equivalently the  $p_- - p_+$ ) phase space. For low  $T$ , we set  $p_- = p_+ = 0$  in  $\mathcal{M}$ . Further, specializing to  $s_1 \approx 0$  simplifies  $\mathcal{M}$  dramatically (only one term of a series remains — see DB80 for details). In this case,  $\mathcal{M} = \mathcal{N}^{(1)} + \mathcal{N}^{(2)}$ , with

$$\begin{aligned}\mathcal{N}^{(1)} &= \frac{2}{B + \omega_1} \left\{ \omega_1 c_1 \epsilon_+^{(2)} \epsilon_-^{(1)} + \omega_2 s_2 \epsilon_z^{(2)} \epsilon_-^{(1)} e^{i\phi_2} \right\} \\ \mathcal{N}^{(2)} &= \frac{2}{B + \omega_2} \left\{ \omega_2 c_2 \epsilon_+^{(1)} \epsilon_-^{(2)} - \omega_2 s_2 \epsilon_z^{(2)} \epsilon_+^{(1)} e^{-i\phi_2} \right\},\end{aligned}\tag{9}$$

and the polarization vector components  $\epsilon_z$ ,  $\epsilon_\pm$  are given in DB80. The integration over azimuthal angle turns out to be trivial, yielding

$$R_{2\gamma}(\omega_1) \approx \int_{-\infty}^{\infty} \frac{dp_-}{\epsilon_-} \int_{-\infty}^{\infty} \frac{dp_+}{\epsilon_+} \Lambda \exp \left\{ -\frac{\omega_2^2 s_2^2}{2B} - \frac{\epsilon_- + \epsilon_+ - 2}{T} \right\}, \tag{10a}$$

where

$$\Lambda = \frac{n_+ n_- c}{32\pi} \frac{\alpha_f^2 \lambda_c^2}{TB} \omega_1 \sum_{\text{pol}} \left\{ |\mathcal{N}^{(1)}|^2 + |\mathcal{N}^{(2)}|^2 \right\}. \tag{10b}$$

Since the pair temperature is low, the integrations over  $p_-$  and  $p_+$  can be performed by the method of steepest descent. However it must be noted that there are two major regions of contribution to these integrals: in the neighbourhood of  $p_- = -p_+ = 0$ , corresponding to  $c_2 = -\omega_1 c_1 / \omega_2$  and  $\omega_2 = 2 - \omega_1$ , and also near  $c_2 = -1$  and  $\omega_2 = 1/\omega_1$ . The total spectrum is, in general, well approximated by the sum of these two contributions.

The contribution  $R_I$  from  $p_\pm \approx 0$  for  $\theta_1 = 0^\circ$  occurs only in the left wing of the line. Evaluation of eq. (10) is then straightforward, resulting in

$$R_I(\omega_1) \approx n_+ n_- c \alpha_f^2 \lambda_c^2 \frac{2\omega_1}{B} \frac{\omega_1^2 - 2\omega_1 + 2}{(B + \omega_1)^2} \exp \left\{ -\frac{2(1 - \omega_1)}{B} \right\}, \quad \omega_1 < 1. \tag{11}$$

This contribution is magnetically broadened, and is generally the dominant contribution when  $T \lesssim B^2$ . It is consistent with the numerical plots, and reproduces the exact cold plasma, zero viewing angle approximation derived in eq. (14) of Kaminker *et al.* (1987). The second component  $R_{II}$ , for  $c_2 \approx -1$ ,  $p_+ \approx 0$  and  $p_- \approx \omega_1 - 1/\omega_1$ , occurs in both wings of the line and is a Doppler broadened contribution. When  $B \lesssim \sqrt{T}$ , eq. (10) gives

$$R_{II}(\omega_1) \approx n_+ n_- c \alpha_f^2 \lambda_c^2 \frac{\omega_1^{3/2}}{\sqrt{\pi T}} \exp \left\{ -\frac{(\omega_1 - 1)^2}{T\omega_1} \right\}, \tag{12}$$

which agrees with the  $B = 0$ , 1D thermal result in eq. (30) of Kaminker *et al.* (1990).

The results in equations (11) and (12), which can be extended to provide a more complicated approximation to the spectrum when  $T \sim B^2$ , indicate that the annihilation line is thermally broadened in the right wing ( $\omega_1 > 1$ ), but both thermally and magnetically broadened in the left wing. This concurs with the numerical results plotted in the figures. The widths obtainable from eqs. (11) and (12) agree with those in eqs. (5) and (7), and from eq. (8) it can be deduced that when  $B \ll 1$ , small temperatures  $T \lesssim B^2/8$  are necessary for magnetic broadening to be important when  $\theta_1 \approx 0^\circ$ . Work is in progress to extend these analytic results to the regime of larger angles  $\theta_1$ .

## CONCLUSIONS

The results presented in this paper show that two-photon annihilation of electrons and positrons with 1D thermal distributions can be significantly influenced by a strong magnetic field. Even for temperatures as high as  $T = 0.1$ , at large viewing angles to the field, magnetic broadening dominates for  $B \gtrsim 10^{12}$  G. More specifically, in gamma-ray burst models where the cooling of pairs by cyclotron resonant scattering is important, the widths of annihilation features seen at viewing angles  $\theta > 45^\circ$  will be determined primarily by the magnetic field. At most viewing angles, the magnetic field preferentially broadens the red side of the annihilation line. An integration over viewing angles removes this asymmetry. Analytic approximations for zero viewing angle are obtained: the spectrum is well-described by a simple sum of magnetically-broadened and Doppler-broadened contributions. For low  $T$ , the numerical computations are found to agree well with the cold annihilation results of Kaminker *et al.* (1987). The results presented in this paper have significant observational implications: the widths and spectral shapes of observed annihilation features in gamma-ray burst and pulsar spectra may provide diagnostics of both the magnetic field strength and viewing angle in these sources.

## REFERENCES

- Agrinier, B., *et al.*: 1990 *Astrophys. J.* **355**, 645  
 Daugherty, J. K., and Bussard, R. W.: 1980 *Astrophys. J.* **238**, 296 (DB80)  
 Harding, A. K.: 1986 *Astrophys. J.* **300**, 167 (Corr. 462)  
 Kaminker, A. D., Pavlov, G. G. and Mamradze, P. G.: 1987 *Astrophys. Sp. Sci.* **138**, 1  
 Kaminker, A. D., Pavlov, G. G. and Mamradze, P. G.: 1990 *Astrophys. Sp. Sci.* **174**, 241  
 Lamb, D. Q., Wang, J. C. L. and Wasserman, I.: 1990 *Astrophys. J.* **363**, 670  
 Liang, E. P.: 1986 *Astrophys. J.* **304**, 682  
 Mazets, E. P., *et al.*: 1981 *Nature* **290**, 378  
 Preece, R. D. and Harding, A. K.: 1991 *Astrophys. J.*, in press.  
 Wunner, G.: 1979 *Phys Rev. Lett.* **42**, 79